Supplementary Information

A combination strategy targeting combustion enhancement for electrically controlled rocket fuel exerts synergistic divestiture against zirconium's electrostatic hazards

Zhiwen Wang[a, b], Feng Li[a, b], Qianyi Zhang[a, b], Keer Ouyang[a, c], Ruiqi Shen[a, b, c], Yinghua Ye[a, b, c], Luigi T. DeLuca[d], Wei Zhang[a, b, c*]

[a] *School of Chemistry and Chemical Engineering, Nanjing University of Science and Technology, Nanjing 210094, China*

[b] *Institute of Space Propulsion, Nanjing University of Science and Technology, Nanjing 210094, China*

[c] *Micro-Nano Energetic Devices Key Laboratory of MIIT, Nanjing 210094, China*

[d] *Space Propulsion Laboratory (SPLab), Department of Aerospace Science and Technology, Politecnico di Milano (RET), Milan, I-20156, Italy*

***Corresponding Author**

Email address: wzhang@njust.edu.cn.

This PDF file includes:

Figs. S1 to S4

Tables S1 to S2

Movie1

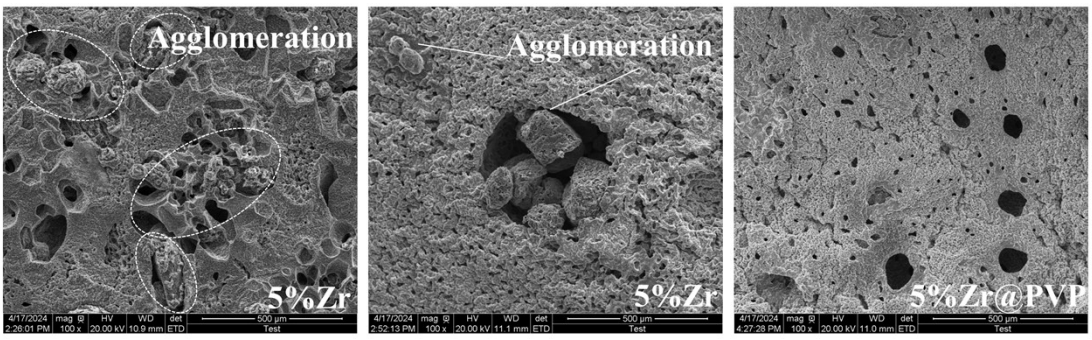

Fig. S1. A broad-range scanning electron microscopy (SEM) for 5%Zr and 5%Zr@PVP.

As depicted in **Fig. S1**, a broad-range scanning electron microscopy (SEM) examination was conducted on the 5%Zr and 5%Zr@PVP propellants to evaluate the dispersion uniformity or aggregation of zirconium in the ECSP. The microscopic morphology indicated that Zr particles coated with PVP, which contained hydrophilic groups, exhibited superior dispersibility during the manufacturing process. In contrast,

the untreated Zr particles tended to agglomerate in the propellant, forming large particles in the order of hundreds of micrometers, which might lead to local unstable deflagration during the combustion process of the propellant.

The kinetic parameters of ECSP were calculated using Kissinger's model and Flynn-wall-Ozawa's model. As shown in **Eq. 1** and **Eq. 2**, the kinetic parameters of the T_{HTD} for 5%Zr@PVP ECSP were calculated using Kissinger and FWO methods.

$$\ln\left(\frac{\beta}{T_p^2}\right) = \ln\left(\frac{AR}{E_a}\right) - \frac{E_a}{RT_p} \tag{1}$$

$$\ln(\beta) = \ln\left(\frac{AR}{Rg(a)}\right) - 5.331 - 1.0516\frac{E_a}{RT_p} \tag{2}$$

Where β is the heating rate (K/min), T_p is the temperature of the exothermic peak (K), A is the pre-exponential factor (s^{-1}), R is the gas constant with 8.314 J/(mol·K) and E_a is the activation energy (J/mol).

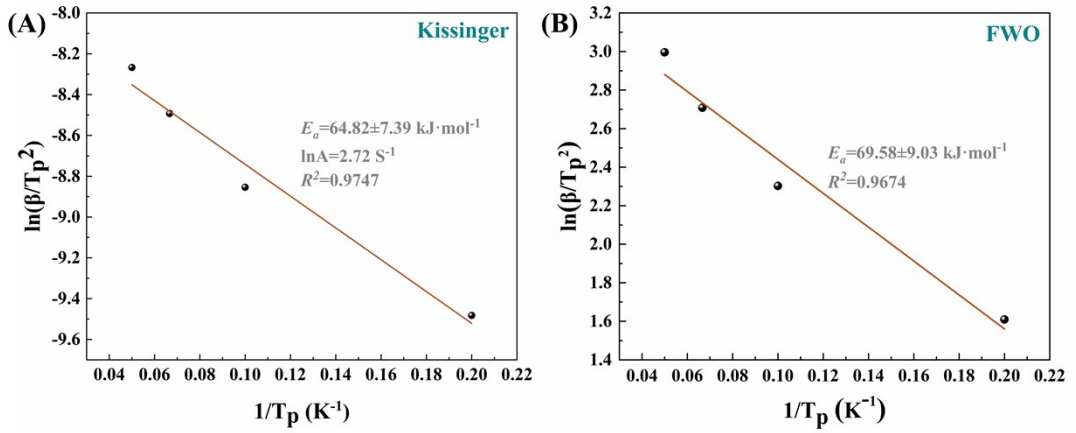

Fig. S2. The kinetic parameters of the T_{HTD} for 5%Zr@PVP ECSP. (A) Kissinger's model. **(B)** Flynn-wall-Ozawa's model.

A comparative analysis of the ESD sensitivity of 5%Zr and 5%Zr@PVP was also conducted, as shown in **Fig. S3**. The ESD sensitivity E_{50} of both propellants was greater than 3215 mJ (the maximum testing capability of the electrostatic sensitivity instrument NJUST-ESD-24), significantly higher than that of Zr@PVP particles. This suggested that the ESD shielding of Zr particles inside the curing propellant by PVP was not the primary factor, but rather water played a dominant role.

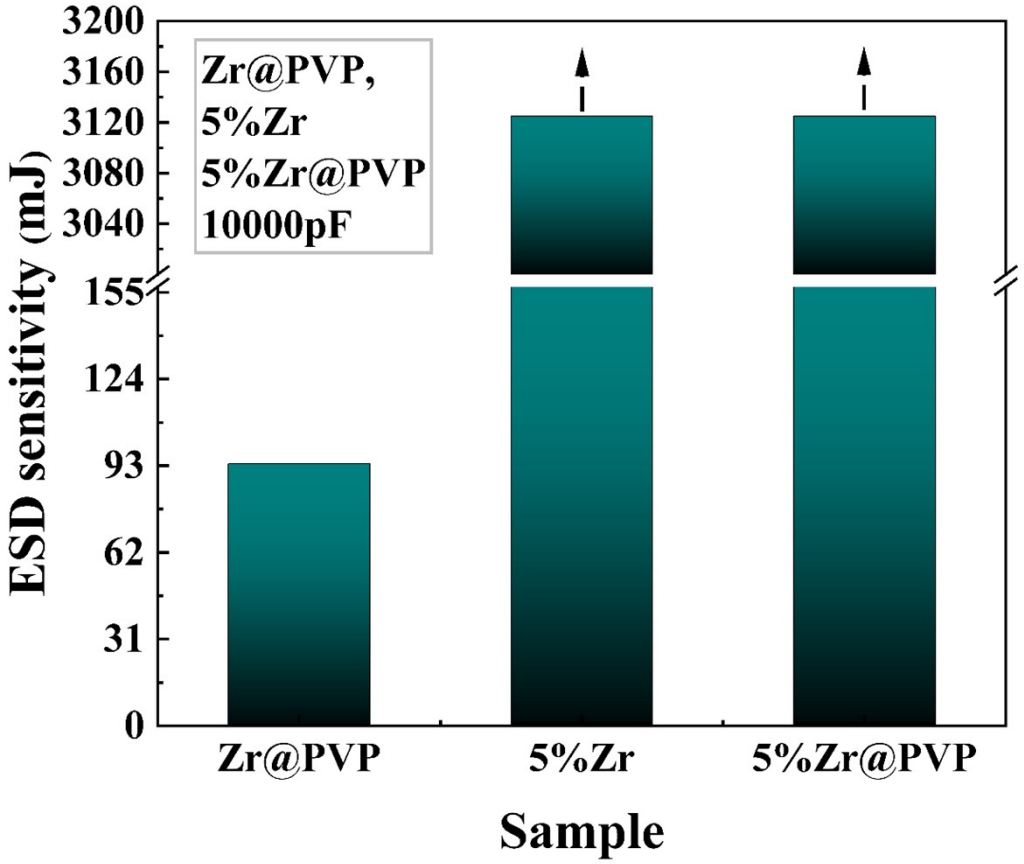

Fig. S3. ESD sensitivity *E50* for Zr@PVP, 5%Zr and 5%Zr@PVP.

Table S1. The combustion characteristics for baseline.

Voltage (V)	Combustion characteristics		
	Ignition delay (ms)	Extinguishment delay (ms)	Burning rate (mm/s)
100	1125	21.25	1.34
125	1030	20.00	1.65
150	678.3	16.75	1.58
175	570.3	6.50	2.53
200	220.7	6.25	2.77

Table S2. The combustion characteristics and regulation capability of burning rate for 5%Zr and 5%Zr@PVP (150V).

Samples	Combustion characteristic (150V)			
	Ignition delay (ms)	Extinguishment delay (ms)	Burning rate (mm/s)	Regulation ratio
5%Zr	1014	19	2.71	1.597
5%Zr@PVP	1003	21	2.76	1.658

Additionally, the combustion characteristics (ignition delay, extinguishment delay,

burning rate, and regulation capability of burning rate) of 5%Zr and 5%Zr@PVP (listed in **Table S2**) were investigated concurrently to assess the potential impact of PVP on the combustion performance of the ECSP. The influence of PVP on the ignition for ECSP was nearly negligible. PVP gradually swelled and dissolved in water during the manufacturing process, aiding in the uniform dispersion of Zr without compromising the energy release of Zr fuel. Besides, the PVP content during the manufacturing of Zr@PVP was minimal to minimize the effect of an excessively thick PVP shell on the energy density and energy release of Zr fuel.

Experimental setup and data processing

Schematic diagram of the sandwich-structured electrode configuration

The sandwich-structured electrode configuration (**Fig. S4**) comprised a mesh anode, propellant, and a flat cathode, enabling real-time dynamic contact between the propellant and both electrodes for stable electrically controlled combustion. A PTFE roller was connected beneath the cathode, ensuring smooth movement of the entire assembly within the bearing.

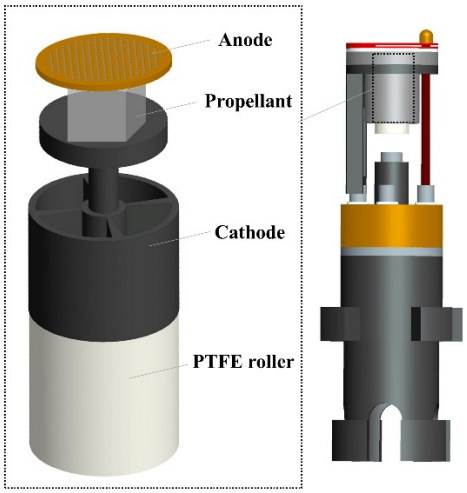

Fig. S4. schematic diagram of the sandwich-structured electrode-propellant-electrode.

Method 1：Comprehensive combustion characteristics based on photoelectric time difference

The combustion process of ECSP can be divided into: i) ignition, ii) combustion, and iii) extinguishment, constituting a cycle. Herein, an ignition-combustion-

extinguishment cycle is referred to a stage. The detailed data processing method is based on photoelectric time difference.[1-5]

The ignition characteristic parameters of ECSP include the nth ignition delay time ($t_{i,n}$). $t_{i,n}$ can be determined by **Eq. (3)**.

$$t_{i,n} = t_{1,n} - t_{0,n} \quad (n = 1,2) \tag{3}$$

where $t_{0,n}$ and $t_{1,n}$ are the moments of when the nth voltage applied and ignition on the propellant surface, respectively.

The combustion characteristic parameters of ECSP include the nth burning rate (r_n) and nth adjustable capability of the burning rate ($AC_{r,n}$). r_n can be determined by **Eq. (4)**.

$$r_n = \frac{\Delta H_n}{t_n} = \frac{\Delta m_n}{\rho S t_n} = \frac{(m_{n-1} - m_n)V}{m_{n-1} S (t_{3,n} - t_{1,n})} \quad (n = 1,2) \tag{4}$$

where m_{n-1} and m_n are the mass of the propellant before and after the nth combustion, respectively. *V* is the volume of the propellant before the nth ignition, and *S* is the contact area between the propellant and the cathode. $t_{2,n}$ and $t_{3,n}$ are the moments when the nth electrical energy is removed from the propellant and the flame on the propellant surface disappears, respectively.

The extinguishment characteristic parameter of ECSP is mainly the nth extinguishment delay time $(t_{e,n})$. $t_{e,n}$ can be determined by **Eq. (5)**

$$t_{e,n} = t_{3,n} - t_{2,n} \quad (n = 1,2) \tag{5}$$

Movie1

Excited-Zr micro-fireballs continuously triggers the combustion propagation of intermediates.

References

1. L. Bao, H. Wang, Z. Wang, H. Xie, S. Xiang, X. Zhang, W. Zhang, Y. Huang, R. Shen and Y. Ye, *Combust. Flame*, 2022, **236**, 111804.
2. L. Bao, H. Wang, T. Zheng, S. Chen, W. Zhang, X. Zhang, Y. Huang, R. Shen

and Y. Ye, *Propellants Explos. Pyrotech.*, 2020, **45**, 1790-1798.

3. L. Bao, W. Zhang, X. Zhang, Y. Chen, S. Chen, L. Wu, R. Shen and Y. Ye, *Combust. Flame*, 2020, **218**, 218-228.
4. F. Li, Z. Wang, Q. Zhang, Z. Cheng, Y. Yu, R. Shen, Y. Ye, L. T. DeLuca and W. Zhang, *Chem. Eng. J.*, 2024, **487**, 150562.
5. Z. Wang, H. Xie, S. Xiang, K. Ouyang, L. Bao, R. Shen, Y. Ye and W. Zhang, *Chem. Eng. J.*, 2023, **456**, 140958.